Ecosystems (2006) 9: 357–373
DOI: 10.1007/s10021-005-0013-x

ECOSYSTEMS

Seasonal Variation in Aboveground Production and Radiation-use Efficiency of Temperate rangelands Estimated through Remote Sensing

Gervasio Piñeiro,* Martín Oesterheld, and José M. Paruelo

Facultad de Agronomía, Departamento de Recursos Naturales y Ambiente, Laboratorio de Análisis Regional y Teledetección (LART), Universidad de Buenos Aires, IFEVA/CONICET, Buenos Aires, Argentina

Abstract

Aboveground net primary production (ANPP) of grasslands varies spatially and temporally. Spectral information provided by remote sensors is a promising new tool that may be able to estimate ANPP in real time and at low cost. The objectives of this study were (a) to evaluate at a seasonal scale the relationship between ANPP and the normalized difference vegetation index (NDVI), (b) to estimate seasonal variations in the coefficient of conversion of absorbed radiation into aboveground biomass (ε_a), and (c) to identify the environmental controls on such temporal changes. We used biomass-based field determinations of ANPP for two grassland sites in the Flooding Pampa, Argentina, and related them with NDVI data derived from the NOAA Advanced Very High Resolution Radiometer (AVHRR) satellites using three different models. Results were compared with data obtained from the new Moderate Resolution Imaging Spectroradiometer (MODIS) sensor at an additional site. The first model was based solely on NDVI; the second was based on the amount of photosynthetically active radiation absorbed by the green vegetation ($APAR_g$), which was derived from NDVI and incoming photosynthetically active radiation (PAR); the third was based on $APAR_g$ and ε_a, which was in turn estimated from climatic variables. NDVI explained between 63 and 93% of ANPP variation, depending on the site considered. Estimates of ANPP were not improved by considering the variation in incoming PAR. At both sites, ε_a varied seasonally (from 0.2 to 1.2 g DM/MJ) and was significantly associated with combinations of precipitation and temperature. Combining ε_a variations with $APAR_g$ increased our ability to account for seasonal ANPP variations at both sites. Our results indicate that NDVI produces good, direct estimates of ANPP only if NDVI, PAR, and ε_a are correlated throughout the seasons. Thus, in most cases, seasonal variations of ε_a associated with temperature and precipitation must be taken into account to generate seasonal ANPP estimates with acceptable accuracy.

Key words: grasslands; radiation-use efficiency; aboveground net primary production; normalized difference vegetation index (NDVI); NOAA Advanced Very High Resolution Radiometer (AVHRR); Moderate Resolution Imaging Spectroradiometer (MODIS); remote sensing; Argentina.

Introduction

Aboveground net primary production (ANPP) varies with season, but such variations are difficult

Received 5 February 2004; accepted 2 March 2005; published online 13 April 2006.
*Corresponding author; e-mail: pineiro@ifeva.edu.ar

to measure due to methodological limitations. Traditional methods for estimating ANPP are based on biomass harvesting, which is expensive and not exempt from errors and methodological problems (Sala and others 1988; Scurlock and others 2002). Due to the time and effort required, ANPP estimates based on biomass harvesting are spatially and temporally limited: data may be obtained for only one or a few places and times and then must be extrapolated. Additionally, differences in the methods used to convert biomass harvests into ANPP may introduce variations of up to 400% in the ANPP value estimated from the same harvests (Scurlock and others 2002). Spectral information generated by coarse-resolution sensors onboard satellites has the potential to be used to estimate ANPP in real time, at low cost, and with full area coverage. However, translating remotely sensed data into ANPP remains a major research challenge. Attempts to do so at an annual time scale have been numerous and successful (Tucker and others 1985; Box and others 1989; Hunt 1994; Gamon and others 1995; Paruelo and others 1997, 2004; Rassmusen 1998; Matsushita and Tamura 2002; Smith and others 2002; Wylie and others 2002; Awaya and others 2004) but only a few studies have correlated seasonal variations in ANPP with spectral indices (Bartlett and others 1989; Nouvellon and others 2000; Paruelo and others 2000).

Several spectral indices that can be used to estimate vegetation variables have been proposed (Choudhury 1987; Baret and Guyot 1991; Ridao and others 1998; Fensholt 2004), but the normalized difference vegetation index (NDVI) is the one most broadly applied. This index integrates two key spectral features of the photosynthetic tissues: their low reflectance in the red wavelengths and their high reflectance in the infrared portions of the electromagnetic spectrum. It is calculated as:

$$\mathrm{NDVI} = (IR - R)/(IR + R)$$

where R is the reflectance in the red portion of the electromagnetic spectrum and IR is the reflectance in the infrared portion.

The NDVI has been directly related to ANPP in many ecosystems (Goward and others 1985; Tucker and others 1985; Box and others 1989; Prince 1991b; Paruelo and others 1997, 2000). However, it has been related more thoroughly with leaf area index (LAI) and, based on this relationship, with the fraction of photosynthetically active radiation absorbed by green vegetation ($FAPAR_g$) (Baret and Guyot 1991; Sellers and others 1992; Gamon and others 1995; Asner 1998; Gower and others 1999; Reeves and others 2001; Nemani and others 2003; Asner and others 2004; Paruelo and others 2004). From the relationship between NDVI and $FAPAR_g$, it is possible to calculate the absorbed photosynthetically active radiation by green vegetation ($APAR_g$) from remote sensing data by multiplying $FAPAR_g$ by the incoming photosynthetically active radiation (PAR), readily available from weather stations. Net primary production (NPP) can then be derived from the Monteith (1972) model:

$$\mathrm{NPP} = \varepsilon_n \left[\int \mathrm{APAR}\right]$$

where ε_n is the energy conversion coefficient (g DM/MJ of $APAR_g$) of absorbed radiation into NPP (Ruimy and others 1999; Running and others 2001). The equation can be modified to estimate ANPP; hence, ε_a can be defined as the energy conversion coefficient of absorbed radiation into ANPP (Field and others 1995).

The theoretical model proposed by Monteith (1972) may be used to estimate the seasonal variation of ANPP from coarse-resolution remotely sensed data as long as the following two issues are resolved: (a) the form of the relationship between NDVI and $FAPAR_g$, and (b) the seasonal variation of ε_a. The form of the relationship between $FAPAR_g$ and NDVI is currently under investigation and varies widely among biomes. Some authors have shown that NDVI saturates at high $FAPAR_g$ values (generally with LAI values higher than 3) (Sellers and others 1994) and hence a nonlinear relationship is expected, whereas the findings of others support a linear relationship (Choudhury 1987; Goward and Huemmrich 1992; Sellers and others 1994). Radiative transfer models show the mechanistic basis of the constraints on the relationship between NDVI and $FAPAR_g$, quantifying the effects of background optical properties, canopy structure, sun/view geometry, chlorophyll content, and so on. This issue has been widely discussed (Verhoef 1984; Baret and Guyot 1991; Sellers and others 1994; Jacquemoud and others 2000; Combal and others 2002; Myneni and others 1997, 2002), although much less attention has been paid to correctly assessing ε_a variations, which probably have much larger impacts on seasonal estimates of NPP from remotely sensed data (Nouvellon and others 2000).

In this study we used empirical approaches to estimate $FAPAR_g$ from NDVI using both a linear and a nonlinear relationship. The description of the

seasonal changes of ε_a is probably more relevant because it has been proven to depend on temperature and on water and nutrient availability (Prince 1991a; Field and others 1995, Gamon and others 1995; Gower and others 1999; Nouvellon and others 2000). Although the relationship between ε_a and these seasonally varying factors is recognized, it has rarely been quantified for grassland ecosystems. Nouvellon and others (2000) estimated ε_a variations at a shortgrass steppe site in Arizona. They pointed to the lack of information and emphasized the importance of estimating this coefficient correctly, particularly in water-limited ecosystems and when seasonal (rather than annual) ANPP needs to be estimated.

From Monteith's conceptual model, it follows that ANPP and NDVI may or may not be directly correlated, depending on the particular relationships among NDVI, $FAPAR_g$, PAR, and ε_a. A strong correlation (either linear or nonlinear) may be expected if ε_a and PAR are constant or vary much less than NDVI over the range of situations in which ANPP is estimated from NDVI, or if they strongly covary with NDVI. These patterns likely explain why NDVI is a good surrogate for ANPP at global and regional scales and on a whole-year basis (Goward and others 1985; Tucker and others 1985; Box and others 1989; Burke and others 1991; Prince 1991b; Paruelo and others 1997; Rassmusen 1998; Potter and others 1999; Seaquist and others 2003). Seasonal variations of both PAR (due to seasonal changes in day length and solar angle) and ε_a (due to changes in temperature, soil water, nutrients, and plant phenology) challenge the ability of NDVI by itself to estimate ANPP at this temporal scale (Bartlett and others 1989; Nouvellon and others 2000). Seasonal calibrations will enable us to explore environmental constraints on ANPP and elucidate the magnitude and importance of each factor throughout the year, mainly by assessing the regional-scale controls of ε_a.

The objectives of this article were (a) to evaluate the relationship between ANPP and NDVI at a seasonal scale, (b) to estimate the seasonal variations in the coefficient of conversion of absorbed radiation into aboveground biomass (ε_a), and (c) to understand the environmental controls on such temporal changes. We used three different models to relate field estimates of ANPP with NDVI obtained from NOAA/Advanced Very High Resolution Radiometer (AVHRR) satellite images. Results were compared with data from the new Moderate Resolution Imaging Spectroradiometer (MODIS) sensor aboard NASA's Terra satellite.

Materials and Methods

Site Description and Field Data

We studied two rangeland sites situated in the northern (Magdalena) (35°20′S, 57°60′W) and southwestern (Laprida) (38°32′S, 61°55′W) portions of the Flooding Pampa in Buenos Aires province, Argentina (Figure 1). The Flooding Pampa is covered almost entirely by rangelands (natural grasslands and sown pastures). The natural grasslands are codominated by C_3 and C_4 grasses of the genera *Stipa*, *Piptochaetium*, *Briza*, *Paspalum*, and *Botriochloa*. A detailed description of these grasslands can be found in Perelman and others (2001) and references therein. The dominant species in the sown pastures are grasses such as *Festuca arundinacea*, *Lolium multiflorum*, and tall wheatgrass (*Agropyron elongatum* or *Elytrigia elongata*), as well as legumes, such as *Trifolium repens, Medicago sativa*, and *Lotus corniculatus*. Mean annual precipitation ranges from 800 to 900 mm, and PAR ranges from 2,600 to 2,900 (MJ/m^2y^{-1}). Precipitation is more abundant in summer, but short periods of drought are common due to the high evaporation rates during this season. Mean temperature varies from 7–10°C in the coldest month (July) to 20–22°C in the warmest month (January). Mollisols are the dominant soils and they are often limited by flooding and alkalinity. Soils are black and are almost entirely covered by vegetation, with only some patches of bare soil. Mean annual ANPP of these different types of grassland is approximately 6,000–8,500 (kg DM ha y^{-1}) (Sala and others 1981; Doll and Deregibus 1986; Oesterheld and León 1987; Rusch and Oesterheld 1997; Paruelo and others 2000).

We used previously published ANPP data for each site. For the northern site (Magdalena), we used measurements (from November 1982 to November 1983) of Oesterheld and León (1987) from three different sown pastures of 2, 5, and 13 years of age. The 13-year-old pasture was considered a natural grassland based on its species composition (León and Oesterheld 1982; Oesterheld and León 1987). Biomass was estimated by harvesting ten random plots of 0.4 m^2. Green and standing dead biomass were separated in the laboratory. Litter was collected manually from the same plots, and all samples were oven dried and weighed with a precision of 0.1 g. ANPP was estimated by considering green to standing dead and standing dead to litter fluxes (for more details, see Sala and others 1981; Oesterheld and León 1987). Variations in harvested biomass within plots were low, with a maximum of 8.0%, a minimum of 2.8%, and an average of 4.7%. In the southwestern site

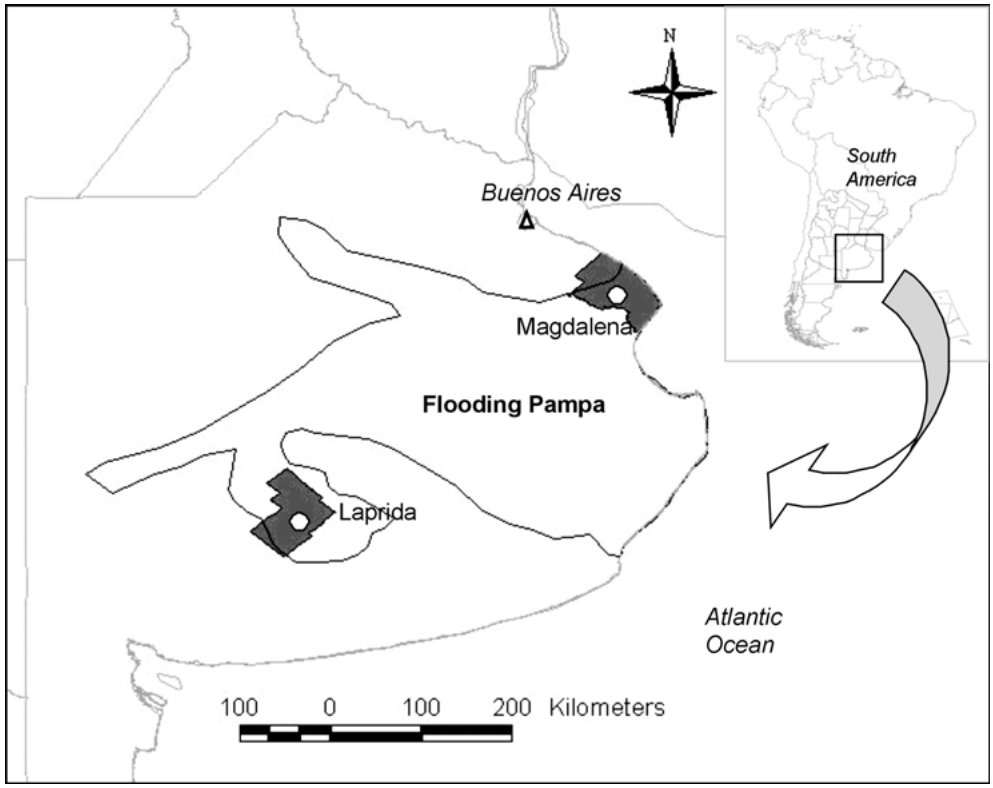

Figure 1. Map of Buenos Aires province, Argentina, showing the Flooding Pampa region and the locations of the study sites in Magdalena and Laprida counties.

(Laprida), we used ANPP data from 1992 to 1995 presented by Paruelo and others (2000) for five rangelands that encompass most of the region's heterogeneity. Eight 1 m^2 plots were randomly situated in each paddock, and ANPP was estimated using wire cages and harvesting at 3 cm height, simulating intense use by livestock. Green and standing dead biomass were oven-dried and weighted. Litter was not collected at this site (see Paruelo and others 2000 for more details).

Spectral Data

We used the NOAA Pathfinder (AVHRR) land data set (1982–2000) of the NDVI released by NASA in 2000. This new data set solved many of the problems detected in the prior NDVI time series developed by NASA (Goward and others 1991; Goward and Huemmrich 1992; Hanan and others 1995, 1997) and includes normalization for variations in the solar zenith angles (see effects in Goward and Huemmrich 1992; Roujean and Breon 1995) and advanced atmospheric corrections to better account for ozone absorption and Rayleigh scattering effects. These changes in image-processing algorithms produced a substantially improved NOAA/AVHRR data set (see http://daac.gsfc.nasa.gov/CAMPAIGN_DOCS/FTP_SITE/readmes/pal.html for detailed information). Unfortunately, no data were available to perform water vapor and aerosol corrections. However, it has been shown that these atmospheric corrections had little effect on NOAA-derived NDVI values in wetlands in Bolivia (Moreau and others 2003) and changed NDVI interannual variations in grasslands of Canada only slightly (Cihlar and others 2004). The data set is made up of 10-day maximum value composites (MVC) of daily NDVI images (Holben 1986), which minimizes negative cloud effects, with a pixel of 64 km^2 (Agbu and James 1994). NDVI values were derived from the reflectance values of channels 1 (red, 580–680 mm) and 2 (infrared, 725–1,100 mm) of the NOAA/AVHRR satellites (for more details, see Agbu and James 1994; James and Kalluri 1994). After extracting pixel values, we calculated monthly maximum values (from the 10-day composites) to avoid low (downward) deviations of NDVI caused by cloud effects and satellite errors not eliminated by the compositing process. After this correction, we performed a visual evaluation of NDVI monthly time series to eliminate extremely high values.

For our analysis, we selected the broadly used NDVI (Steven and others 2003), although several recent indexes have been considered to perform better than NDVI under bare soil conditions (Roujean and Breon 1995; Fensholt 2004) or very dense canopies (usually for LAI higher than 3 or 4,

common in forest or crops) (Asner and others 2004; Haboudane and others 2004). But these situations do not apply to the grasslands of this study. For example, the correlation between NDVI and the new enhanced vegetation index (EVI), both derived from the new MODIS satellites, was found to be higher than 0.90 ($n = 22$, $P < 0.01$) for 22 grassland pixels of the study region during four different years (G. Piñeiro unpublished).

Data Aggregation

We related field estimates of ANPP with NDVI values acquired over the same period. We extracted pixel values from two target areas (one in each site), which were delineated to avoid agricultural lands. According to Argentinean agricultural statistics, only a very small portion of the target area in Magdalena was under cropping during the period studied (1982–1983 = 3.3% and 1983–1984 = 2.1%), and almost all the land was covered by natural grasslands and sown pastures (http://www.sagpya.mecon.gov.ar). Hence, we defined the target area in Magdalena from eight pixels that overlaid the field plots. By contrast, agriculture was important in Laprida. Thus, we used maps of grassland and crop areas generated by Guerschman and others (2003) from LANDSAT TM images. We selected seven NOAA/AVHRR pixels around the measurement sites with less than 10% agriculture. NDVI values of the pixels within each target area were very similar (mean coefficient of variation for all dates was 4% in Magdalena and 5% in Laprida), which reflects the homogeneity of the areas. We averaged the NDVI values of the pixels of each target area and computed monthly NDVI time series.

ANPP series were constructed by a weighted average of field measurements based on the proportion of rangeland types in each target area. Based on our field experiences, we considered that 50% of Magdalena was covered by natural grasslands and 50% by sown pastures (25% 2-year-old pastures and 25% 5-year-old pastures). Considering this rangeland cover, we calculated a weighted average from Oesterheld and León's (1987) data and generated a bimonthly time series of ANPP for the entire target area. For our analysis in Laprida, we used a similar approach, but we classified the five pastures into three classes according to their productivity: high-productivity pastures, low-productivity pastures, and tall wheatgrass with natural grasslands. Based on Guerschman and others (2003) land-cover classification, we estimated the proportion of each rangeland class in the whole target area and calculated a weighted average ANPP series. Variations in the actual proportions of rangeland types will not affect paper outcomes because ANPP was similar among grassland types.

Model Development and Assessment of ANPP and ε_a

For each site and for the two sites combined, we evaluated the proportions of the seasonal variance of ANPP explained by three increasingly complex models (Figure 2). The first, the NDVI model, consisted of a simple regression model of ANPP-NDVI, whereas the second and third, the APAR and the Epsilon models, were based on Monteith's (1972) rationale.

The NDVI model (Figure 2) postulates that the seasonal variation in ANPP may be accounted for by NDVI. Thus, it assumes that PAR, $APAR_g$, and ε_a either are constant or strongly covary with NDVI. We generated a model through regressions between observed values of ANPP and NDVI derived from the databases described above.

In the APAR model (Figure 2), seasonal variations in ANPP may be accounted for by $APAR_g$. In contrast to the NDVI model, the APAR model may better account for seasonal variations in ANPP when NDVI and PAR are partially uncoupled. However, ε_a is assumed to be either constant or correlated with $APAR_g$. The model was generated through regressions between observed ANPP values and estimates of $APAR_g$, calculated as the product of PAR and $FAPAR_g$. $FAPAR_g$ was estimated from NDVI according to the three different methods outlined in the introduction and described in detail below.

In the Epsilon model (Figure 2), seasonal changes in ANPP depend on $APAR_g$ and ε_a dynamics. Some authors relate gross primary production (GPP) with $APAR_g$ and ε_g instead of NPP with $APAR_g$ and ε_n, and include respiration costs in the right side of equation (Goetz and others 1999; Liu and others 2002; Matsushita and Tamura 2002; Hazarika and others 2005). When measurements of NPP or ANPP are performed in the field, it is not necessary to estimate respiration because NPP or ANPP can be directly related to $APAR_g$ (Potter and others 1993; Gower and others 1999; Ruimy and others 1999; Turner and others 2002; Medlyn and others 2003; Paruelo and others 1997, 2004). Discrimination of respiration cost represents an advantage in models developed across biomes because respiration costs vary among biomes. However, within a single biome, respiration costs would be held nearly constant. For these two reasons, we used the NPP model where respiration costs are

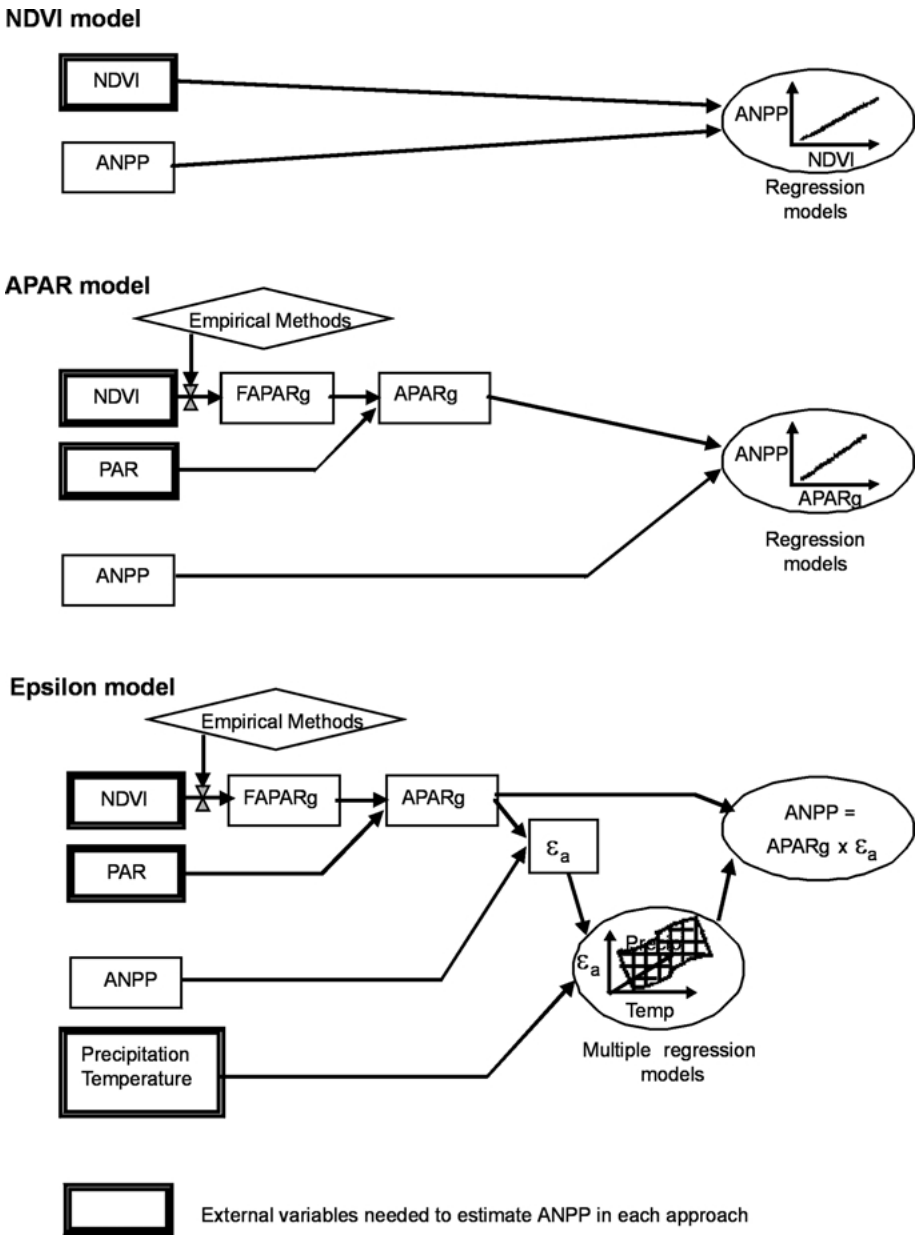

Figure 2. Diagrammatic representation of the calibration process followed in the three models used to estimate aboveground net primary production (ANPP), based on remotely sensed data and climate variables. In the evaluation process, new regression models for ANPP and the coefficient of conversion of absorbed radiation into aboveground biomass (ε_a) were generated using part of the data set, and their ANPP predictions were evaluated against independent data. NDVI, normalized difference vegetation index; $APAR_g$, photosynthetically active radiation absorbed by green vegetation; PAR, photosynthetically active radiation; $FAPAR_g$, fraction of photosynthetically active radiation absorbed by green vegetation.

included in ε_a (Running and others 2001). A critical point for applying the Epsilon model is to derive estimates of seasonal changes in ε_a. Thus, we analyzed the climatic controls on ε_a using multiple regression analysis. We calculated ε_a from the ratio between field values of ANPP and $APAR_g$ estimates, which was calculated from NDVI and PAR as described below. The climatic variables were obtained from daily values of precipitation recorded at the ranches where ANPP was measured and daily values of temperature recorded at nearby weather stations (Colonia and Dolores).

We derived $FAPAR_g$ from NDVI by using three semi-empirical methods widely used in the literature: (a) a linear relationship between $FAPAR_g$ and NDVI proposed by Choudhury (1987), Goward and Huemmrich (1992), Ruimy and others (1994), and Moreau and others (2003) (hereafter referred to as the ''linear method''); (b) a nonlinear relationship between $FAPAR_g$ and NDVI proposed by Potter and others (1993), Sellers and others (1994), and Paruelo and others (1997) (hereafter referred to as the ''nonlinear method''); and (c) the average of the two previous methods as proposed by Los and others (2000) (hereafter referred to as the ''combined method'').

In the case of the linear method, we set maximum NDVI as the 98th percentile of the time series.

Maximum NDVI (0.70) was similar for both areas and was set to 95% of $FAPAR_g$ interception, assuming saturation at high LAI values. Bare soil NDVI ($FAPAR_g = 0$) was assumed to be 0.01. We obtained the following equation: $FAPAR_g = [\min (1.38 \times NDVI - 0.014), 0.95]$. For the nonlinear method, we directly followed Potter and others (1993), who recommended a maximum and minimum NDVI = 0.67 and 0.004, respectively, which are equivalent to $SR_{max} = 5.13$ and $SR_{min} = 1.08$. SR is the simple ratio index = (1 + NDVI)/(1 − NDVI) = R/IR. The resulting equation was: $FAPAR_g = \min [SR / (SR_{max} - SR_{min}) - SR_{min} / (SR_{max} - SR_{min}), 0.95]$. This equation results in a nonlinear relationship between NDVI and $FAPAR_g$ and accounts for the widely described saturation of NDVI at high LAI (greater than 3) (Baret and Guyot 1991; Sellers and others 1992; Los and others 2000; Asner and others 2004).

Model Evaluation

To evaluate the three models against independent data, we developed new regression models using part of the ANPP data set. We used these models to make predictions that were contrasted with observed ANPP values not used to generate the models. Due to restrictions in data availability, only the models for both sites combined were evaluated. In each case, 16 values were used for model generation and 5 values were used for model evaluation. We repeated this procedure five times with different random combinations of data used for model generation and evaluation (Manly 1997). For data analyses, we used SAS 8.2, *proc reg*, and *proc rsquare* procedures.

We further evaluated the Epsilon model by applying it to a different data set with ANPP measured at La Carola farm near the Laprida site and NDVI obtained from the MODIS sensor. Compared to the NOAA/AVHRR data set, MODIS images have better geometric and radiometric performance and multispectral characteristics, thus enabling complete atmospheric corrections that increase data quality significantly (Myneni and others 2002; Fensholt 2004; Running and others 2004). However, because the MODIS sensor has only been functioning since 2000, temporal series analysis was restricted. The new analysis was performed at La Carola farm (37°20′S, 61°30′W) near the Laprida site, where estimates of ANPP were taken in the same manner as described for Laprida, but for the years 2001 and 2002. We retrieved 16-day composites of NDVI from the MODIS 250 × 250 m images for the same periods that ANPP was measured, and we estimated $FAPAR_g$ from NDVI using a nonlinear equation generated from maximum and minimum SR values, as for the NOAA images. Maximum SR value ($SR_{max} = 10.77$) was estimated by the 98th percentile of grassland pixels; minimum SR ($SR_{min} = 1.54$) was estimated by the 5th percentile of bare soil pixels. $FAPAR_g$ estimated from MODIS-NDVI was multiplied by incident PAR recorded at a nearby weather station to provide monthly $APAR_g$. Seasonal variations of ε_a were calculated by dividing ANPP by $APAR_g$ and were compared with ε_a calculated by the multiple regression equation obtained from the NOAA images. Precipitation data necessary to estimate ε_a were obtained from daily values recorded at La Carola, and daily temperature was recorded at a nearby weather station. We used field ANPP values measured at La Carola to evaluate ANPP estimates calculated as the product of MODIS-$APAR_g$ and ε_a estimated with the equations that had been obtained from the NOAA/AVHRR images using multiple regression models.

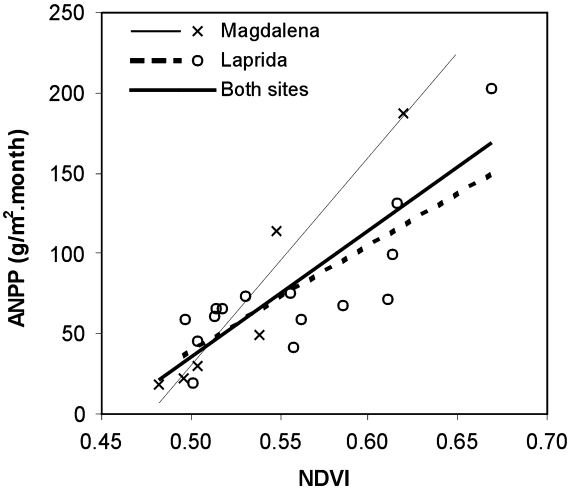

Figure 3. Linear relationships between Aboveground net primary production (ANPP) and the normalized difference vegetation index (NDVI) (the NDVI model), for each site and for both sites together. For Magdalena, ANPP = 1,303 × NDVI − 622; $r^2 = 0.93$. For Laprida, ANPP = 667 × NDVI − 295; $r^2 = 0.65$. For both sites together, ANPP = 791 × NDVI−360; $r^2 = 0.68$. All regressions are significant at $P < 0.01$.

Results

The NDVI model showed different relationships between sites. ANPP and NDVI were strongly correlated at the Magdalena site ($r^2 = 0.93$, $P < 0.01$, $n = 6$) (Figure 3). The relationship was weaker in Laprida ($r^2 = 0.65$, $P < 0.01$, $n = 15$) or when the

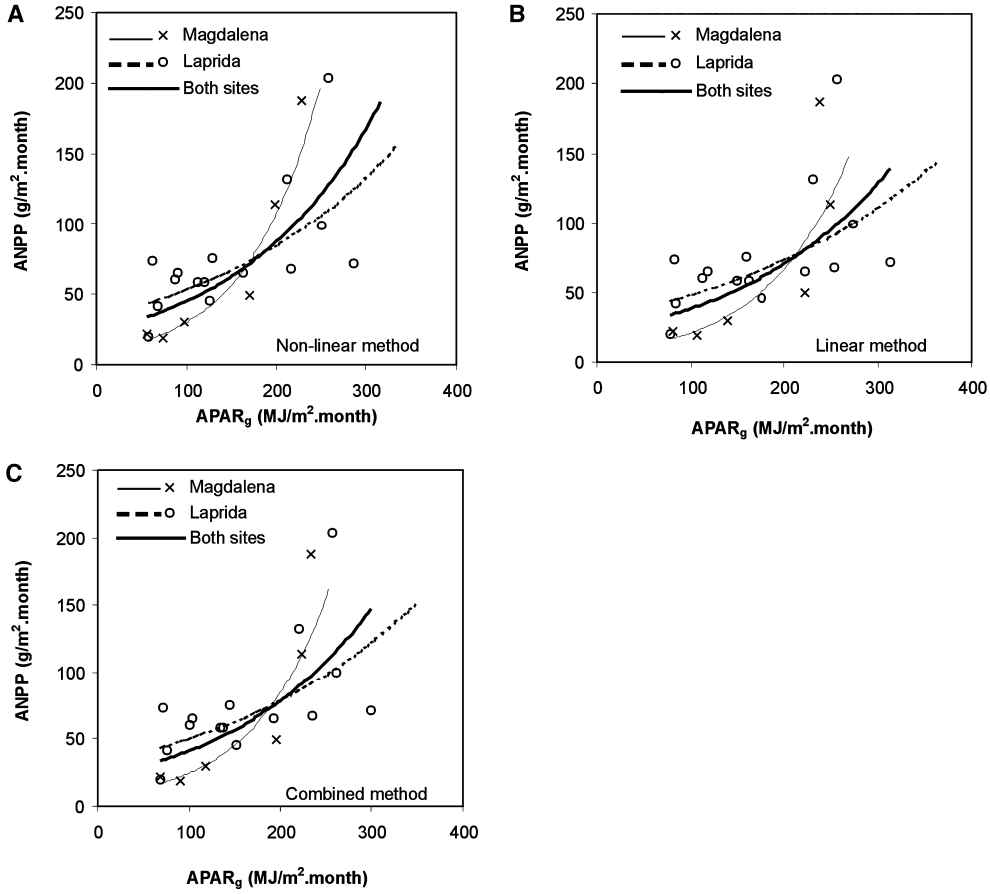

Figure 4. Exponential relationships between ANPP and photosynthetically active radiation absorbed by green vegetation ($APAR_g$) (the APAR model), for each site and for both sites pooled. $APAR_g$ was derived from $FAPAR_g$ values and PAR. $FAPAR_g$ was estimated from NDVI based on the nonlinear method (**A**), the linear method (**B**), and the combined method (**C**). Regression equations when $FAPAR_g$ was estimated by the nonlinear method were as follows: for Magdalena ANPP = $8.50 \times e^{0.013 \times APAR_g}$, r^2= 0.94; for Laprida ANPP = $33.73 \times e^{0.0046 \times APAR_g}$, r^2= 0.46; for both sites together ANPP = $23.32 \times e^{0.0066 \times APAR_g}$, r^2 = 0.55. Regression equations when $FAPAR_g$ was estimated by the linear method were as follows: for Magdalena ANPP = $6.59 \times e^{0.012 \times APAR_g}$, r^2 = 0.82; for Laprida ANPP = $31.81 \times e^{0.0042 \times APAR_g}$, r^2 = 0.37; and for both sites together ANPP = $20.96 \times e^{0.0060 \times APAR_g}$, r^2= 0.46. Regression equations when $FAPAR_g$ was estimated by the combined method were as follows: for Magdalena ANPP = $7.26 \times e^{0.012 \times APAR_g}$, r^2 = 0.80; for Laprida ANPP = $32.42 \times e^{0.0044 \times APAR_g}$, r^2 = 0.41; and for both sites together ANPP = $21.77 \times e^{0.0064 \times APAR_g}$, r^2 = 0.51. All regressions were significant at $P < 0.01$. $FAPAR_g$, fraction of photosynthetically active radiation absorbed by green vegetation; PAR, photosynthetically active radiation.

data from both sites were pooled (r^2 =0.68, $P < 0.01$, $n = 21$). Slopes were not significantly different between sites ($P = 0.21$), but intercepts differed ($P < 0.05$). Linear models between ANPP and NDVI showed the best fit for all the cases, but exponential models also fit the data well (r^2 = 0.90, 0.58, and 0.65 for Magdalena, Laprida, and the pooled database, respectively).

The APAR model did not explain a significantly higher proportion of the seasonal variation of ANPP than the NDVI model, even though one more variable was added (PAR) (Figure 4). As in the previous model, the Magdalena site had a higher r^2 than Laprida and than both sites taken together (Figure 4). In contrast to the NDVI model, exponential functions fit the data better than linear functions. When $FAPAR_g$ was calculated using the nonlinear method, the proportion of ANPP accounted for by $APAR_g$ was higher than when it was calculated by the linear or the combined method.

Before showing the results for the Epsilon model, we first need to show the results on radiation-use efficiency (ε_a) and its relation with climatic variables, which were inputs to that model. We found that ε_a, as estimated from the ratio between field estimates of ANPP and $APAR_g$, varied sea-

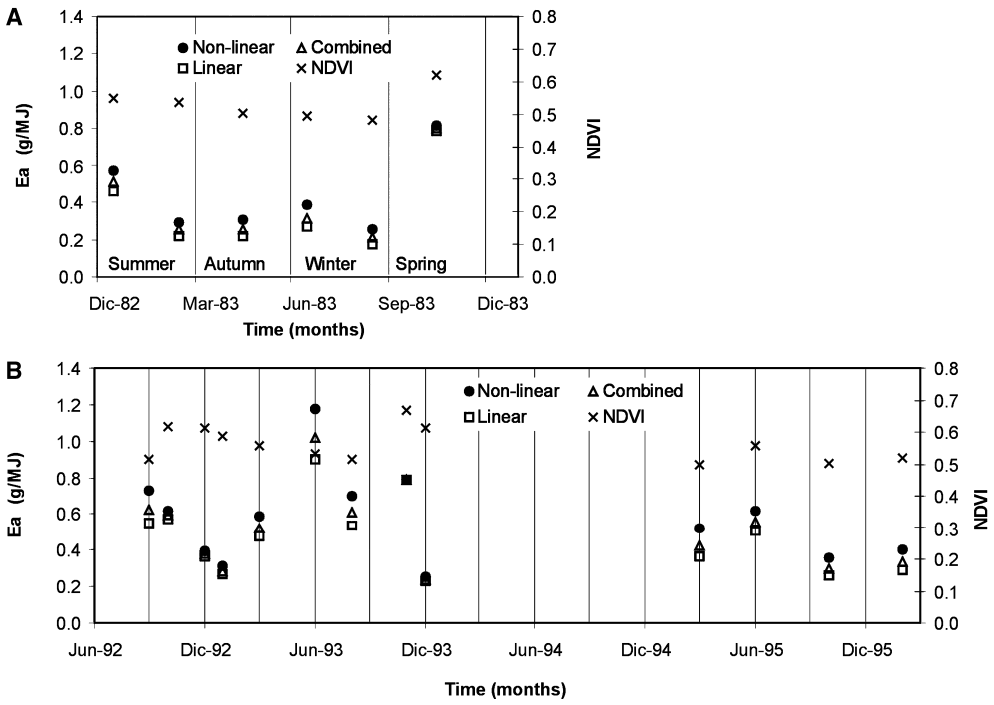

Figure 5. Seasonal changes in the coefficient of conversion of absorbed radiation into aboveground biomass (ε_a) and NDVI. **A** Magdalena and **B** Laprida. We calculated ε_a as ANPP/$APAR_g$, with $APAR_g$ derived from the nonlinear method (*solid circles*), the linear method (*open squares*), or the combined method (*open triangles*). *Crosses* (×) show NDVI in the second axis. ANPP, aboveground net primary production; $APAR_g$, photosynthetically active radiation absorbed by green vegetation.

sonally between 0.2 and 1.2 g DM/MJ. The range of values was similar for both sites (Figure 5). Generally, ε_a values were higher in winter and lower in summer, but periods of high rainfall or drought increased or decreased ε_a, respectively, in all months. Precipitation and temperature were the main controls on ε_a variations. At relatively low values of NDVI, the ε_a values derived using the nonlinear method to estimate $FAPAR_g$ were higher than those derived using the linear method because the former method predicts lower $FAPAR_g$ values than the latter one. However, for high NDVI values, both methods converged due to the similar $FAPAR_g$ estimates (Figure 5). As expected, the combined method produced intermediate values of ε_a. Differences among methods were small, resulting in only 9% variation in ε_a estimates.

Temperature and precipitation accounted for a substantial proportion of the seasonal variability of ε_a, but the importance of each variable changed among sites. Precipitation (PP) was significantly correlated with ε_a at all sites, but precipitation anomalies (PPAN = [monthly precipitation − mean precipitation] / mean precipitation) accounted for a larger proportion of ε_a variations than precipitation (Table 1). For Magdalena and both sites together, temperature was not significantly associated with ε_a. In contrast, temperature and ε_a were significantly related in Laprida (Table 1). Multiple regression models using precipitation and temperature as independent variables improved ε_a estimates for Laprida and for both sites pooled together, but not for Magdalena. For both sites together, mean monthly minimum temperatures (TMIN) increased the variance explained by PPAN from 0.49 to 0.58 (mean of the three methods for estimating $FAPAR_g$ from NDVI) (Table 2). In Laprida, the multiple regression model that accounted for most of the ε_a variations included PP instead of PPAN and mean monthly maximum temperatures (TMAX) (Table 2), although PPAN had a higher r^2 than PP in the simple models (Table 1).

The Epsilon model yielded a consistently higher r^2 than the other models both for the individual sites and the pooled database. The r^2 obtained in the calibration of these models ranged from 0.97 to 0.99 (depending on the method used for computing $FAPAR_g$ from NDVI) for Magdalena, from 0.84 to 0.90 for Laprida, and from 0.87 to 0.93 for both sites pooled together. The nonlinear method always fit the data better, but differences were insignificant. The three methods used to estimate $FAPAR_g$ from NDVI produced similar ANPP estimates (on average ±9%), and the combined method always resulted in intermediate values. However, at high ANPP, differences in estimated ANPP among methods were larger (19%).

Correlations among NDVI, PAR, $APAR_g$, and ε_a at each site help to explain the results obtained by the three different models. At Magdalena, the three models performed well because all the variables were highly correlated (Table 3). On the other

Table 1. Simple Linear Regression Models of ε_a as the Dependent Variable and Climatic Data as Independent Variables

	r^2			Slope			*y*-intercept		
Variable	Non-L	Lin	CM	Non-L	Lin	CM	Non-L	Lin	CM
Magdalena (n = 6)									
PP	0.81	0.84	0.83	0.048	0.052	0.050	−0.046	−0.072	−0.013
PPAN	0.85	0.89	0.88	0.37	0.34	0.36	0.40	0.32	0.36
Laprida (n = 15)									
PP	0.13	0.22	0.17	0.025	0.028	0.026	0.38	0.26	0.32
PPAN	0.47	0.45	0.47	0.26	0.21	0.24	0.56	0.45	0.50
TMEAN	0.30	0.21	0.26	−0.030	−0.021	−0.025	1.01	0.77	0.89
TMAX	0.35	0.26	0.31	−0.028	−0.020	−0.024	1.15	0.88	1.01
TMIN	0.23	NS	0.20	−0.030	NS	−0.025	0.83	NS	0.73
Both sites (n = 21)									
PP	0.20	0.31	0.25	0.029	0.033	0.031	0.31	0.19	0.25
PPAN	0.49	0.50	0.50	0.27	0.24	0.26	0.51	0.42	0.46

Non-L, Non-linear; Lin, linear; CM, combined method; PP, monthly precipitation (in cm); PPAN, monthly precipitation anomalies: (observed precipitation–mean precipitation)/mean precipitation; TMEAN, mean monthly temperature (°C); TMAX, mean monthly maximum temperature (°C); TMIN, mean monthly minimum temperature (°C). Only significant variables ($P < 0.10$) are shown.

Table 2. Best Multiple Linear Regression Models of ε_a as the Dependent Variable and Climatic Data as Independent Variables

	r^2_{adj}			Slope			Intercept		
Variable	Non-L	Lin	CM	Non-L	Lin	CM	Non-L	Lin	CM
Laprida									
PP	0.64	0.65	0.66	0.042	0.040	0.041	1.04	0.78	0.91
TMAX				−0.037	−0.029	−0.033			
Both sites									
PPAN	0.61	0.55	0.59	0.28	0.25	0.26	0.82	0.63	0.72
TMEAN				−0.020	−0.014	−0.017			

Non-L, nonlinear; Lin, linear; CM, combined method; PP, monthly precipitation (in cm); PPAN, monthly precipitation anomalies: (observed precipitation–mean precipitation)/mean precipitation; TMEAN, mean monthly temperature (°C); TMAX, mean monthly maximum temperature, (°C).
For Magdalena there was not a significant multiple regression model.
All variables and both models are significant at $P < 0.01$.

hand, correlations were weaker in Laprida and for both sites pooled together; hence, the three models achieved different results with these two databases. It is interesting to note that the direction of the correlations between PAR and $APAR_g$ with ε_a varied between sites. It is probable that the paucity of data available at Magdalena is generating these differences.

Evaluation of the models against independent data (only performed for both sites pooled together) showed that the Epsilon model generated more stable and reliable estimates. For this model, the coefficients constructed with different subgroups of data were particularly similar (Table 4, coefficient of variation), indicating relatively high model stability. The NDVI model presented less stable coefficients. When evaluated against independent data, the NDVI and the APAR models estimated ANPP with lower accuracy than the Epsilon model (Figure 6). The APAR model also underestimated productivity at high values. The epsilon model was the only one that estimated well the highest, unusual ANPP values. These two extreme values (see Figure 6) increased the r^2 of the regression model, but r^2 was still high and significant if they were eliminated ($r^2 = 0.57$). For the other models, r^2 dropped to 0.20 and 0.31 when these values were removed.

Seasonal ε_a variations derived from the equations presented in Table 4 correlated well with ε_a estimates generated from new ANPP data at La Carola farm and APARg derived from the MODIS sensor

Table 3. Cross-correlations between Variables Registered for Each Site Separately and for Both Sites Pooled Together

	Magdalena (n = 6)	Laprida (n = 15)	Both Sites (n = 21)
NDVI vs PAR	0.69	0.54	0.56
NDVI vs ε_a	0.90–0.93	−0.02–0.24	0.24–0.46
PAR vs ε_a	0.47–0.48	−0.42–(−0.56)	−0.15–(−0.30)
$APAR_g$ vs ε_a	0.64–0.76	−0.30–(−0.39)	−0.02–(−0.10)

NDVI, normalized difference vegetation index; PAR, photosynthetically active radiation; ε_a, coefficient of conversion of absorbed radiation into aboveground biomass; $APAR_g$, photosynthetically active radiation absorbed by green vegetation.
Correlations including ε_a show the range of correlations obtained with the three methods for estimating the fraction of photosynthetically active radition absorbed by green vegetation ($FAPAR_g$) from NDVI—the nonlinear, the linear, and the combined method.

Table 4. Coefficients of Determination and Model Parameters of the ANPP and ε_a Regressions Performed with Different Sets of Data

	r^2	a	b	c
NDVI model: ANPP = a + NDVI × b				
Set 1	0.67	−400	856	
Set 2	0.74	−358	802	
Set 3	0.52	−193	479	
Set 4	0.67	−375	820	
Set 5	0.74	−375	817	
Mean	0.67	−340	755	
Conf. Int.	±0.08	±73	±136	
STD	0.09	84	156	
CV (%)	13	25	21	
APAR model: ANPP = a × $\exp^{(APARg \times b)}$				
Set 1	0.48	21.5	0.0061	
Set 2	0.39	24.2	0.0056	
Set 3	0.32	28.9	0.0041	
Set 4	0.49	20.3	0.0063	
Set 5	0.49	18.9	0.0066	
Mean	0.43	22.8	0.0057	
Conf. Int.	±0.07	±3.46	±0.0009	
STD	0.08	3.95	0.0010	
CV (%)	18	17	17	
Epsilon model: ε_a = a + PPAN × b + TMEAN × c				
Set 1	0.73	0.69	0.29	−0.014
Set 2	0.67	0.74	0.27	−0.016
Set 3	0.60	0.74	0.24	−0.018
Set 4	0.59	0.76	0.29	−0.018
Set 5	0.60	0.63	0.28	−0.012
Mean	0.64	0.71	0.27	−0.016
Conf. Int.	±0.05	±0.05	±0.02	±0.002
STD	0.06	0.05	0.02	0.003
CV (%)	9	7	8	17

NDVI, normalized difference vegetation index; ANPP, aboveground net primary production; APAR, photosynthetically active radiation absorbed by green vegetation; PPAN, monthly precipitation anomalies; TMEAN, mean monthly temperature; Conf. Int., confidence interval; STD, standard deviation; CV, coefficient of variation.
All models are significant at $P < 0.05$.
Data sets were generated by randomly extracting five values from the entire data set (both sites pooled together).
For the APAR and Epsilon models, the fraction of photosynthetically active radition absorbed by green vegetation ($FAPAR_g$) was derived from NDVI using the non-linear method.

(r = 0.74, n = 11, $P < 0.01$) (Figure 7), in spite of the different spatial resolutions of the NOAA (8 × 8 km) and MODIS (250 × 250 m) images. Both the measured ε_a (MODIS-derived) and the estimated ε_a at La Carola showed similar seasonal variations when compared to the values obtained with NOAA images

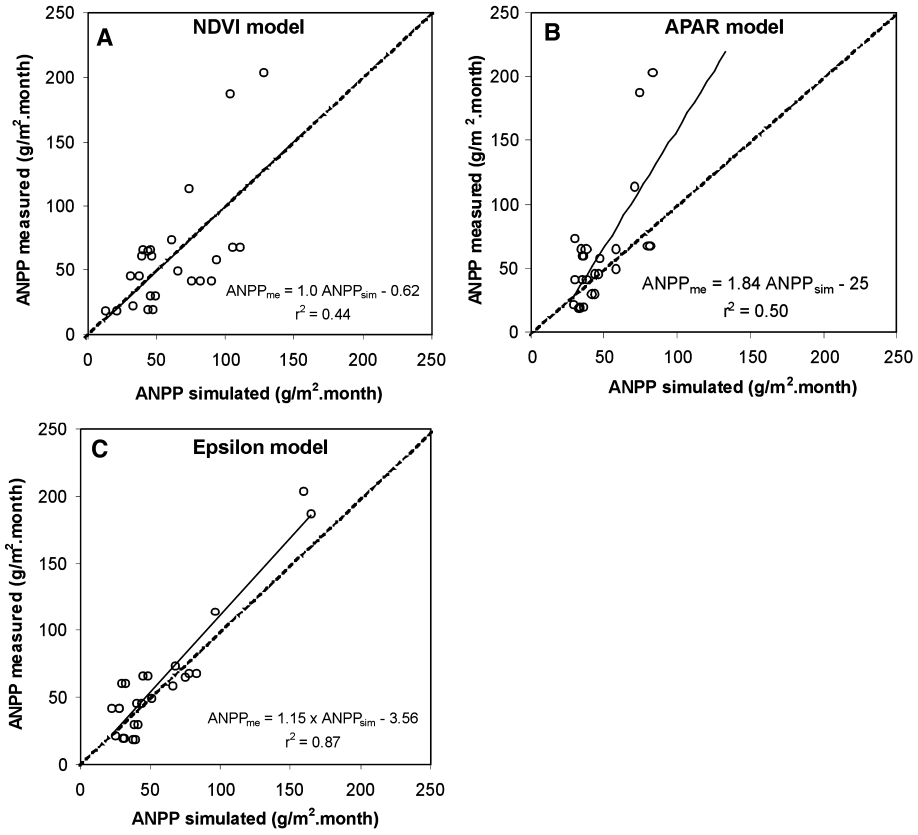

Figure 6. Relationships between measured vs simulated ANPP using three different models. (**A**) NDVI model. (**B**) APAR model. (**C**) Epsilon model. For method used to calculate ANPP, see the equations in Table 4. Data are for both sites pooled together. For the APAR and Epsilon models, $FAPAR_g$ was estimated from NDVI based on the nonlinear method. Simulated ANPP was estimated with data not included in the generation of the models.

at Magdalena and Laprida: They were at maximum in late winter or early spring and minimum in summer. Low and insignificant correlation between ε_a and ANPP is obvious in this graph (Figure 7) ($r < 0.2$, $n = 11$, $P > 0.72$). The ANPP calculated from $APAR_g$ derived from the MODIS sensor and ε_a estimated from the equation in Table 4 generated by the NOAA/AVHRR images showed good agreement with the field measurement of ANPP at La Carola farm ($r^2 = 0.90$, $n = 11$, $P < 0.01$).

Discussion

Our results show that low-resolution satellites provide an effective means of tracking seasonal variations in ANPP, but it requires some consideration to selecting the proper model to describe the relationship between spectral indices and ANPP for a specific site or region. The applicability of various simple regression models based on NDVI depends on the strengths of the correlations among NDVI, PAR, and ε_a. In the case of the Magdalena site, because NDVI was seasonally correlated with both PAR and ε_a (Table 3), a simple model relating ANPP and NDVI was adequate to track ANPP dynamics ($r^2 = 0.93$) (Figure 3). Physiologically, this means that green leaf area and PAR interception (and likewise $APAR_g$) are coupled with light-use efficiency. However, this condition is not always met in perennial grasslands, as shown in Laprida. At this site, NDVI was not correlated with ε_a, so a more mechanistic model (the Epsilon model) substantially improved our ability to track ANPP variations. Because NDVI was seasonally correlated with PAR at our two sites (Table 3), the APAR model did not improve the ability to track seasonal variations in ANPP. Furthermore, for each site and the two sites pooled together, the linear regressions between ANPP and $APAR_g$ explained a lower proportion of the ANPP variances than using NDVI alone. Similar results were obtained by Rassmusen (1998), who obtained better and more consistent estimates of rangeland annual NPP in Senegal by using NDVI instead of $APAR_g$.

Due to the lack of direct measurements of $FAPAR_g$, it remains uncertain whether the inclusion of ε_a accounts for real light use efficiency variations (hypothesis 1) or accounts for the limited sensitivity of NDVI at large values of $FAPAR_g$ and ANPP (hypothesis 2). Two lines of evidence support the first hypothesis. First, the same equation is used to compute ε_a at high or low rainfall, and ε_a variations improved ANPP estimates not only at high but also

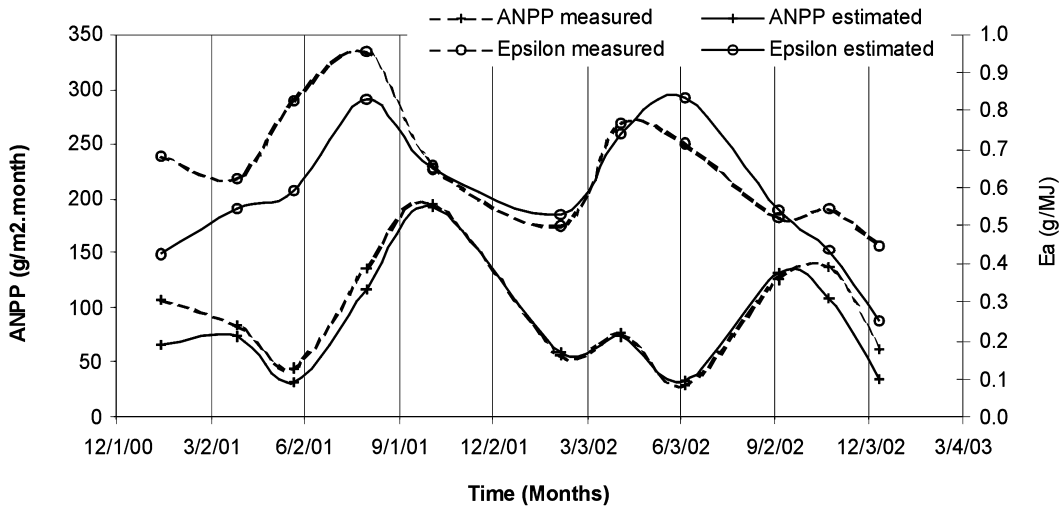

Figure 7. Seasonal variations of measured and estimated values for the coefficient of conversion of absorbed radiation into aboveground biomass (ε_a) and ANPP at La Carola farm. Measured ANPP was estimated in the field by sequential biomass harvests. Estimated ANPP was calculated based on Monteith's rationale, based on NDVI from MODIS images, daily measurements of photosynthetically active radiation (PAR), and ε_a calculated from precipitation and temperature data, using the equation generated from the NOAA/AVHRR images (see Table 4). Measured ε_a was calculated as measured ANPP divided by $APAR_g$ as estimated from the MODIS images. Estimated ε_a was computed using the equation generated from the NOAA/AVHRR images (see Table 4).

at low ANPP values (Figure 6). If the second hypothesis were true, then the Epsilon model would not improve ε_a estimates at low $FAPAR_g$ or ANPP values. Second, the Epsilon model improved ANPP estimates not only with the linear method but also with the nonlinear method which accounts for NDVI saturation better.

The Epsilon model not only was more accurate in estimating ANPP (Figure 6), it also had an important advantage: It can be used with NDVI data from a different sensor, as long as the relationship between $FAPAR_g$ and NDVI is established for each sensor. This is an important advantage because $FAPAR_g$ is easier to measure than ε_a or ANPP. The strength of this approach is based on the description of ε_a dynamics from climate variables. Thus, reliable estimates of ε_a enable the use of multisensor information to derive ANPP time series so that better and more comprehensive data sets can be obtained—for example by coupling ANPP series derived from NOAA/AVHRR and MODIS sensors (Running and others 2004). The difference in spatial resolution between the two images did not change ε_a estimates, probably due to the similarity of the grasslands in the area studied with the NOAA/AVHRR (8 $\times$ 8 km) to the type of grassland at La Carola farm. However, for heterogeneous patches of vegetation, ε_a is expected to change at different spatial resolutions. Finally, if we consider that the radiometric quality of the MODIS sensor is much better than the NOAA/AVHRR sensor (Fensholt 2004), our results imply that the errors expected in the NOAA/AVHRR series due to the lack of a complete atmospheric correction and inferior radiometric performance, are actually small.

Our results also provide independent estimates of ε_a for these rangelands and showed their relationship with seasonal variations in climate, which adds substantially to our limited knowledge on this key aspect of rangeland functioning (Bartlett and others 1989; Prince 1991a; Gamon and others 1995; Churkina and Running 1998; Gower and others 1999; Nouvellon and others 2000). Our ε_a values (annual mean ε_a = 0.42 and 0.52 g DM/MJ, for the linear and nonlinear methods, respectively) fall within the estimates of other authors for the grassland biome. For example, Paruelo and others (1997) estimated the annual ε_a for a wide range of grasslands across the US Great Plains. They found that ε_a = 0.23 g of carbon/MJ $\cong$ 0.48 g DM/MJ. On the other hand, Ruimy and others (1994), in an extensive review of ε_a for different biomes, reported only three estimates for temperate grasslands, with a relatively high mean ε_a of 0.84 g DM/MJ. Field and others (1995) compared values of ε generated from different global models—the CASA and Miami NPP/GCM APAR model. Considering a below-aboveground primary production ratio equal to 1.3 and a coefficient for conversion of carbon into dry matter of 2.22 (Ajtay and others

1979), these models produced ε_a values of 0.26 and 0.45 g DM/MJ, respectively. Estimates of ε_a for North and South American rangelands were quite similar. Further studies are needed to explore the similarities and differences in climatic and biotic controls on the seasonal and annual dynamics of ε_a. In addition, $FAPAR_g$ field measurements, jointly with ANPP, are needed to decrease uncertainties in ε_a estimates. Hyperspectral remote sensing could be used in the near future to derive ε_a estimates directly from remote sensing data (Gamon and others 1992; Smith and others 2002; Asner and others 2004); however, the availability of continuous airborne or satellite-derived hyperspectral images is still restricted to a few places.

The relationship between ε_a and climatic variables presented here provides critical empirical evidence to show that ANPP can be described from remotely sensed data. We found that precipitation was the main control of ε_a throughout the year whereas temperature played a secondary role, probably because it was correlated with PAR. Several authors have developed theoretical models to estimate ε_a from climate and soil variables (Potter and others 1993; Ruimy and others 1994; Field and others 1995; Goetz and others 1999; Seaquist and others 2003), but none of them has evaluated these models against field data at a seasonal scale. In these previous studies, precipitation generally was positively related with ε_a, as we found. These authors also assume that ε_a has an optimum response curve to temperature. However, in the rangelands that we studied, quadratic models did not fit the data better than linear models. It is notable that, whereas temperature in Magdalena was not related to ε_a, in Laprida and for both sites together temperature increments reduce the conversion efficiency (Table 1). This finding can be explained by the elevated PAR values registered in months with high temperatures. The correlation between temperature and PAR (more than 89% in our sites) in natural ecosystems makes it difficult to study their effects on ε_a separately in field studies.

The selection of different empirical relationships between vegetation indices and $FAPAR_g$ had a relatively small effect on $APAR_g$ estimates and, hence, in deriving both ε_a and ANPP. Our results indicate that the nonlinear method is a more accurate way to estimate ANPP, but differences detected among methods in these grasslands were quite small. Unfortunately, we did not have $FAPAR_g$ measurements to verify whether the nonlinear method also yielded better estimates of this variable, which would likely account for the saturation of NDVI at high $FAPAR_g$ values (corresponding generally with LAI values greater than 3) (Baret and Guyot 1991; Goward and Huemmrich 1992; Sellers and others 1994; Haboudane and others 2004). The correct assessment of ε_a variations based on precipitation and temperature data seemed to have larger effects on the accurate estimatation of ANPP than the different methods used to estimate $FAPAR_g$. The latter had an average effect of only 9% on ANPP estimations, with a maximum of 19%, whereas ε_a had an average effect of 27%, with a maximum of 165% (comparing the APAR model to the Epsilon model) (Figure 6).

The estimation of $FAPAR_g$ from NDVI may be improved by the use of radiative transfer models, which take vegetation and soil optical properties into account (Baret and Guyot 1991; Goward and Huemmrich 1992; Sellers and others 1994; Roujean and Breon 1995; Hanan and others 1997; Asner 1998). However, the use of radiative transfer models to derive biophysical variables is not exempt from computational problems (Combal and others 2002), and they have in some cases overestimated $FAPAR_g$ values (Le Roux and others 1997; Fensholt and others 2004). Moreover, although their use would enable a more thorough assessment of the relationship between vegetation indices and $FAPAR_g$, it limits the applicability of our method for estimating ANPP because these models have several practical limitations at broad scales (for example, it is difficult to obtain field values of leaf angle, chlorophyll content, and so on, for natural grasslands that contain more than 100 species in a single square meter). In the near future, radiative transfer models could be more applicable, thanks to the introduction of new multi-angle remote sensors capable of providing some of the parameters needed to characterize canopy architecture (for example, the foliage clumping index) (Bicheron and Leroy 1999; Chen and others 2003). By now, near-linear relationships between vegetation indices and $FAPAR_g$ have been reported widely (Bartlett and others 1989; Sellers and others 1994; Gamon and others 1995; Le Roux and others 1997; Gower and others 1999; Myneni and others 2002; Turner and others 2002; Wylie and others 2002). In grasslands, this relationship is altered more by soil reflectance than by canopy architecture (Roujean and Breon 1995; Asner 1998). The grasslands studied in this paper have almost 100% vegetation cover; hence, soil effects are minimized.

The development of models based on spectral indices capable of estimating ANPP will improve our understanding of forage dynamics and ultimately make it possible to monitor forage resources

easily, rapidly, and at low cost. Over large areas, regional associations of ranchers could apply these estimates to modify their own forage budget models and to improve herbage usage and farm planning. The ability to describe ANPP and ε_a variations within and between years will expand our knowledge of grassland carbon cycling and energy exchange—two key features in any assessment of the impact of global change on these biomes (Field and others 1995; Churkina and Running 1998; Bondeau and others 1999; Gower and others 1999; Potter and others 1999). Our results could also be used as inputs to global NPP models such as CASA (Field and others 1995) or Biome-BGC (Nemani and others 2003) and would improve the ε_a variations currently included in these models. Indeed, they show that the ε_a of perennial grasslands is probably more variable throughout the seasons than is now assumed by these models.

Conclusions

Our research indicates that:

1. Low-resolution satellites can be used to accurately track seasonal variations in ANPP.
2. Depending on the correlation structure of the relevant variables (NDVI, $APAR_g$, ε_a), such tracking may be based simply on NDVI, or it may require estimates of ε_a, which in turn require estimates of $APAR_g$.
3. Seasonal variations in ε_a can be estimated using meteorological data from weather stations. These estimates could then be used with $APAR_g$ data derived from different sensors.
4. The outcome of the ANPP estimates in the study was more sensitive to ε_a variations than to the differences among the specific methods used to estimate $APAR_g$. Therefore, more effort should be focused on identifying the environmental controls on ε_a than on determining the exact shape of the relationship between $FAPAR_g$ and NDVI.

Acknowledgements

This research was partially funded by the Inter-American Institute for Global Change (ISP III-077 and SGP 004); the University of Buenos Aires under the Proyecto Estrategico (Res.(CS) N° 5988/01); the Regional Fund for Agricultural Technology (FONTAGRO) (IICA/BID FTG/RF 0103RG), and the Fondo para la Investigación Científica y Tecnológica (FONCYT) (PICT 99-080671). Gervasio Piñeiro is currently a Ph.D. candidate funded by Consejo Nacional de Investigaciones Científicas y Tecnológicas (CONICET), Argentina. Ricardo Romero from INIA-Uruguay provided valuable climate data, and Gonzalo Grigera helped in retrieving ANPP and remote sensing data. We thank Consorcios Regionales de Experimentación Agrícola (CREA)-Sudoeste for carrying out ANPP measurements. We are also grateful to Kathleen Farley for revising a previous version of this manuscript.

References

Agbu PA, James ME. 1994. The NOAA/NASA Pathfinder AVHRR land data set user's manual. Greenbelt (MD): Goddard Distributed Active Archive Center, NASA, Goddard Space Flight Center.

Ajtay GL, Ketner P, Duvigneaud P. 1979. Terrestrial primary production and phytomass. In: Bolin B, Degens ET, Kempe S, Ketner P, Eds. The global carbon cycle. New York: Willey, p 129–82.

Asner GP. 1998. Biophysical and biochemical sources of variability in canopy reflectance. Remote Sens Environ 64: 234–53.

Asner GP, Nepstad D, Cardinot G, Ray D. 2004. Drought stress and carbon uptake in an Amazon forest measured with spaceborne imaging spectroscopy. Proc Natl Acad Sci USA 101:6039–44.

Awaya Y, Kodani E, Tanaka K, Liu J, Zhuang D, Meng Y. 2004. Estimation of the global net primary productivity using NOAA images and meteorological data: changes between 1988 and 1993. Int J Remote Sen 25:1597–613.

Baret F, Guyot G. 1991. Potentials and limits of vegetation indices for LAI and APAR assessment. Remote Sens Environ 35:161–73.

Bartlett DS, Whiting GJ, Hartman JM. 1989. Use of vegetation indices to estimate indices to estimate intercepted solar radiation and net carbon dioxide exchange of a grass canopy. Remote Sens Environ 30:115–28.

Bicheron P, Leroy M. 1999. A method of biophysical parameter retrieval at global scale by inversion of a vegetation reflectance model. Remote Sens Environ 67:251–66.

Bondeau A, Kicklighter DW, Kaduk J, The Participants of the Potodam NPP Model Intercomparison. 1999. Comparing global models of terrestrial net primary productivity (NPP): importance of vegetation structure on seasonal NPP estimates. Global Change Biol 5:35–45.

Box EO, Holben BN, Kalb V. 1989. Accuracy of the AVHRR vegetation index as a predictor of biomass, primary productivity and net CO_2 flux. Vegetation 80:71–89.

Burke IC, Kittel TGF, Lauenroth WK, Snook P, Yonker CM, Parton WJ. 1991. Regional analysis of the central Great Plains. BioScience 41:685–92.

Chen JM, Liu J, Leblanc SG, Lacaze R, Roujean J-L. 2003. Multi–angular optical remote Sensl for assessing vegetation structure and carbon absorption. Remote Sen Environ 84:516–25.

Choudhury BJ. 1987. Relationships between vegetation indices, radiation absorption, and net photosynthesis evaluated by a sensitivity analysis. Remote Sen Environ 22:209–33.

Churkina G, Running SW. 1998. Contrasting climatic controls on the estimated productivity of global terrestrial biomes. Ecosystems 1:206–15.

Cihlar J, Latifovic R, Chen J, Trishchenko A, Du Y, Fedosejevs G, Guindon B. 2004. Systematic corrections of AVHRR image composites for temporal studies. Remote Sens of Environ 89:217–33.

Combal B, Baret F, Weiss M, Trubuil A, Macé D, Pragnère A, Myneni R, and others. 2002. Retrieval of canopy biophysical variables from bidirectional reflectance: using prior information to solve the ill-posed inverse problem. Remote Sens of Environ 84:1–15.

Doll UM, Deregibus VA. 1986. Efecto de la exclusion del pastoreo sobre el subsitema subterraneo de un pastizal templado humedo. Turrialba 36:337–44.

Fensholt R. 2004. Earth observation of vegetation status in the Sahelian and Sudanian West Africa: comparison of Terra MODIS and NOAA AVHRR satellite data. Int J Remote Sen 25:1641–59.

Fensholt R, Sandholt I, Rasmussen MS. 2004. Evaluation of MODIS LAI, fAPAR and the relation between fAPAR and NDVI in a semi-arid Environ using in situ measurements. Remote Sen Environ 91:490–507.

Field CB, Randerson JT, Malmstrom CM. 1995. Global net primary production: combining ecology and remote Sensl. Remote Sen Environ 51:74–88.

Gamon JA, Penuelas J, Field CB. 1992. A narrow-waveband spectral index that tracks diurnal changes in photosynthetic efficiency. Remote Sens Environ 41:35–44.

Gamon JA, Field CB, Goulden ML, Griffin KL, Hartley AE, Joel G, Penuelas J, and others. 1995. Relationships between NDVI, canopy structure, and photosynthesis in three Californian vegetation types. Ecol Appl 5:28–41.

Goetz SJ, Prince SD, Goward SN, Thawley MM, Small J. 1999. Satellite remote Sensing of primary production: an improved production efficiency modeling approach. Ecol Model 122:239–55.

Goward SN, Huemmrich KF. 1992. Vegetation canopy PAR absorbance and the normalize difference vegetation index: an assessment using the SAIL model. Remote Sens of Environ 39:119–40.

Goward SN, Tucker SJ, Dye DG. 1985. North American vegetation patterns observed with the NOAA–7 Advanced Very High Resolution Radiometer. Vegetation 64:3–14.

Goward SN, Markham B, Dye DG, Dulaney W, Yang J. 1991. Normalized difference vegetation index measurements from the Advanced Very High Resolution Radiometer. Remote Sens Environ 35:257–77.

Gower ST, Kucharik CJ, Norman JM. 1999. Direct and indirect estimation of leaf area index, fAPAR and net primary production of terrestrial ecosystems. Remote Sens Environ 70: 29–51.

Guerschman JP, Paruelo JM, DiBella C, Giallorenzi MC, Pacín F. 2003. Land cover classification in the Argentine pampas using multi-temporal Landsat TM data. Int J Remote Sens 24:3381–402.

Haboudane D, Miller JR, Pattey E, Zarco-Tejada PJ, Strachan IB. 2004. Hyperspectral vegetation indices and novel algorithms for predicting green LAI of crop canopies: modeling and validation in the context of precision agriculture. Remote Sens Environ 90:337–52.

Hanan NP, Prince SD, Begue A. 1995. Estimation of absorbed photosynthetically active radiation and vegetation net production efficiency using satellite data. Agric For Meteorol 76:259–76.

Hanan NP, Begue A, Prince SD. 1997. Errors in remote Sensing of intercepted photosynthetically active radiation: an example from HAPEX–Sahel. J Hydrol 188–9:676–96.

Hazarika MK, Yasuoka Y, Ito A, Dye D. 2005. Estimation of net primary productivity by integrating remote Sensing data with an ecosystem model. Remote Sens of Environ 94:298–310.

Holben B. 1986. Characteristics of maximum value composite images from temporal AVHRR data. Int J Remote Sens 7:1417–34.

Hunt ER. 1994. Relationship between woody biomass and PAR conversion efficiency for estimating net primary production from NDVI. Int J Remote Sens 15:1725–30.

Jacquemoud S, Bacour C, Poilve H, Frangi J-P. 2000. Comparision of four radiative transfer models to simulate plant canopies reflectance: direct and inverse mode. Remote Sens Environ 74:471–81.

James ME, Kalluri SNV. 1994. The pathfinder AVHRR land data set: an improved coarse resolution data set for terrestrial monitoring. Int J Remote Sens 15:3347–63.

León RJC, Oesterheld M. 1982. Envejecimiento de pasturas implantadas en el norte de la Depresion del Salado. Un enfoque sucesional. Rev Facul Agron 3:41–9.

Le Roux X, Gauthier H, Begue A, Sinoquet H. 1997. Radiation absorption and use by humid savanna grassland: assessment using remote Sensl and Model. Agric For Meteoro 85:117–32.

Liu J, Chen JM, Cihlar J, Chen W. 2002. Net primary productivity mapped for Canada at 1 km resolution. Global Ecol Biogeogr 11:115–29.

Los SO, Collatz GJ, Sellers PJ, Malmstrom CM, Pollack TS, DeFries RS, Bounoua L, and others. 2000. A global 9-yr biophysical land surface dataset from NOAA AVHRR data. J Hydrometeorol 1:183–99.

Manly BJF. 1997. Randomization, bootstrap and Monte Carlo methods in biology. 2nd ed. London: Chapman & Hall.

Matsushita B, Tamura M. 2002. Integrating remotely sensed data with an ecosystem model to estimate net primary productivity in East Asia. Remote Sens Environ 81:58–66.

Medlyn B, Barrett D, Landsberg J, Sands P, Clement R. 2003. Conversion of canopy intercepted radiation to photosynthate: review of Model approaches for regional scales. Funct Plant Bio 30:153–69.

Monteith JL. 1972. Solar radiation and productivity in tropical ecosystems. J Appl Ecol 9:747–66.

Moreau S, Bosseno R, Gu XF, Baret F. 2003. Assessing the biomass dynamics of Andean bofedal and totora high–protein wetland grasses from NOAA/AVHRR. Remote Sens of Environ 85:516–29.

Myneni RB, Nemani RR, Running SW. 1997. Estimation of global leaf area index and absorbed Par using radiative transfer models. IEEE Trans Geosci Remote Sens 35:1380–93.

Myneni RB, Hoffman S, Knyazikhin Y, Privette JL, Glassy J, Tian Y, Wang Y, and others . 2002. Global products of vegetation leaf area and fraction absorbed PAR from year one of MODIS data. Remote Sens of Environ 83:214–31.

Nemani RR, Keeling CD, Hashimoto H, Jolly WM, Piper SC, Tucker CJ, Myneni R, and others. 2003. Climate-driven increases in global terrestrial net primary production from 1982 to 1999. Science 300:1560–63.

Nouvellon Y, Lo Seen D, Rambal S, Bégué A, Moran MS, Kerr Y, Qi J. 2000. Time course of radiation use efficiency in a

shortgrass ecosystem: consequences for remotely sensed estimation of primary production. Remote Sens of Environ 71:43–55.

Oesterheld M, León RJ. 1987. El envejecimiento de las Pasturas Implantadas: su efecto en la productividad primaria. Turrialba 37:29–35.

Paruelo JM, Epstein HE, Lauenroth WK, Burke IC. 1997. ANPP estimates from NDVI for the central grassland region of the US. Ecology 78:953–8.

Paruelo JM, Oesterheld M, Di Bella M, Arzadum M, Lafontaine J, Cahuepé M, Rebella C. 2000. Estimation of primary production of subhumid rangelands from remote Sensing data. Appl Veg Sci 3:189–95.

Paruelo JM, Garbulsky MF, Guerschman JP, Jobbágy EG. 2004. Two decades of normalized difference vegetation index changes in South America: identifying the imprint of global change. Int J Remote Sens 25:2793–806.

Perelman SB, León RJC, Oesterheld M. 2001. Cross-Scale vegetation patterns of Flooding Pampa grasslands. J Ecol 89:562–77.

Potter CS, Randerson JT, Field CB, Matson PA, Vitousek PM, Mooney HA, Klooster SA. 1993. Terrestrial ecosystem production: a process model based on global satellite and surface data. Global Biogeochem Cycles 7:811–41.

Potter CS, Klooster S, Brooks V. 1999. Interanual variability in terrestrial net primary production: exploration of trends and controls on regional to global scales. Ecosystems 2:36–48.

Prince SD. 1991a. A model of regional primary production for use with coarse resolution satellite data. Int J Remote Sens 12:1313–30.

Prince SD. 1991b. Satellite remote Sensing of primary production: comparison of results for Sahelian grasslands 1981–1988. Int J Remote Sens 12:1301–11.

Rassmusen MS. 1998. Developing simple, operational, consistent NDVI–vegetation models by applying Environal and climatic information. Part I. Assessment of net primary production. Int J Remote Sens 19:97–117.

Reeves MC, Winslow JC, Running SW. 2001. Mapping weekly rangeland vegetation productivity using MODIS algorithms. J Range Manage 54:90–105.

Ridao E, Conde J, Mínguez I. 1998. Estimating fAPAR from nine vegetation indices for irrigated and nonirrigated faba bean and semileafless pea canopies. Remote Sens Environ 66:87–100.

Roujean J-L, Breon F-M. 1995. Estimating PAR absorbed by vegetation form bidirectional reflectance measurements. Remote Sens Environ 51:375–84.

Ruimy A, Saugier B, Dedieu G. 1994. Methodology for the estimation of terrestrial net primary production from remotely sensed data. J Geophysi Res 99:5263–83.

Ruimy A, Kergoat L, Bondeau A, T.P.O.T.P.N.M. Intercomparison. 1999. Comparing global models of terrestrial net primary productivity (NPP): analysis of differences in light absorption and light-use efficiency. Global Change Biol 5:56–64.

Running SW, Thorton PE, Nemani RR, Glassy JM. 2001. Global terrestrial gross and net primary productivity from the earth observing system. In: Sala OE, Jackson RB, Mooney HA, Howarth RW, Eds. Methods in ecosystem science. Berlin Heidelberg New York: Springer.

Running SW, Nemani RR, Heinsch FA, Zhao M, Reeves MC, Hashimoto H. 2004. A continuous satellite-derived measure of global terrestrial primary production. Bioscience 54:547–60.

Rusch G, Oesterheld M. 1997. Relationship between productivity, and species and functional group diversity in grazed and non–grazed pampas grassland. Oikos 78:519–26.

Sala O, Deregibus V, Schlichter T, Alippe H. 1981. Productivity dynamics of a native temperate grassland in Argentina. J Range Manage 34:48–51.

Sala OE, Biondini ME, Lauenroth WK. 1988. Bias in estimates of primary production: an analytical solution. Ecol Model 44:43–55.

Scurlock JMO, Johnson K, Olson RJ. 2002. Estimating net primary productivity from grassland biomass dynamics measurements. Global Change Biol 8:736–53.

Seaquist JW, Olsson L, Ardöc J. 2003. A remote Sensing-based primary production model for grassland biomes. Ecol Model 169:131–55.

Sellers PJ, Berry JA, Collatz GJ, Field CB, Hall FG. 1992. Canopy reflectance, photosynthesis, and transpiration. III. A reanalysis using improved leaf models and a new canopy integration scheme. Remote Sens of Environ 42:187–216.

Sellers PJ, Tucker CJ, Collatz GJ, Los SO, Justice CO, Dazlich DA, Randall DA. 1994. A global 1° by 1° NDVI data set for climate studies. Part 2. The generation of global fields of terrestrial biophysical parameters from the NDVI. Int J Remote Sens 15:3519–45.

Smith M-L, Ollinger SV, Martin ME, Aber JD, Hallett RA, Goodale CL. 2002. Direct estimation of aboveground forest productivity through hyperspectral remote Sensing of canopy nitrogen. Ecol appl 12:1286–302.

Steven MD, Malthus TJ, Baret F, Xu H, Chopping MJ. 2003. Intercalibration of vegetation indices from different sensor systems. Remote Sens Environ 88:412–22.

Tucker CJ, Vanpraet CV, Sharman MJ, Van Ittersum G. 1985. Satellite remote Sensing of total herbaceous biomass production in the Senegalese Sahel: 1980–1984. Remote Sens of Environ 17:233–49.

Turner DP, Gower ST, Cohen WB, Gregory M, Maiersperger TK. 2002. Effects of spatial variability in light use efficiency on satellite-based NPP monitoring. Remote Sens of Environ 80:397–405.

Verhoef W. 1984. Light scattering by leaf layers with applications to canopy reflectence Model: the SAIL model. Remote Sens of Environ 16:125–41.

Wylie BK, Mayer DJ, Tieszen LL, Mannel S. 2002. Satellite mapping of surface biophysical parameters at the biome scale over North American grasslands: a case study. Remote Sens of Environ 79:266–78.